LANGMUIR

pubs.acs.org/Langmuir Article

Extensive Polymerization of Atomically Precise Alloy Metal Clusters During Solid-State Reactions

Published as part of Langmuir virtual special issue "2023 Pioneers in Applied and Fundamental Interfacial Chemistry: Santanu Bhattacharya".

B. S. Sooraj,[‖] Jayoti Roy,[‖] Manish Mukherjee, Anagha Jose, and Thalappil Pradeep*

Cite This: https://doi.org/10.1021/acs.langmuir.4c01737 Read Online

ACCESS | Metrics & More | Article Recommendations | Supporting Information

ABSTRACT: Exploring the reactions between atomically precise metal clusters and the consequences of such reactions has been an exciting field of research during the past decade. Initial studies in the area were on reactions between clusters in the solution phase, which proceed through the formation of dimers of reacting clusters. In the present work, we examine the interaction between two atomically precise clusters, $[Au_{25}(PET)_{18}]^-$ and $[Ag_{25}(DMBT)_{18}]^-$, in the solid state, where PET and DMBT are 2-phenylethanethiol and 2,4-dimethylbenzenethiol, respectively. The experiments were performed using different ratios of these two clusters, and it was inferred that the kinetics of the reactions were faster compared with reactions in the solution. The metal exchange between these two clusters, due to their interactions in the solid state, leads to the formation of dimers, trimers, tetramers, and polymers of atomically precise alloy metal clusters. We observed polymer entities up to hexamers, which were observed for the first time. Control experiments revealed that metal exchange is a key factor leading to polymerization. Our work points to a new approach for synthesizing polymers of atomically precise alloy metal clusters.

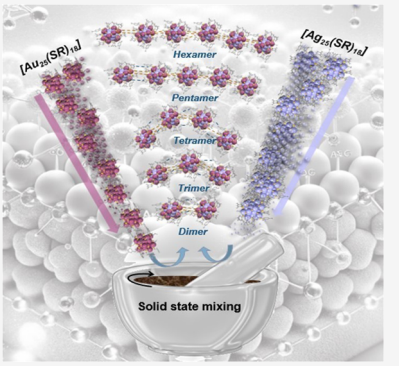

INTRODUCTION

Atomically precise metal clusters are a class of molecules that are well-known for their diverse properties.[1−8] Their structural integrity, composition, and electronic confinement make them promising candidates for various applications.[9−12] Over the past decade, exploring the reactions between atomically precise metal clusters has evolved as a new research area of interest. These reactions in the solution phase and in the gas phase have been probed using mass spectrometry.[13−16] In such reactions, the exchange of metal atoms and ligands occurs, while maintaining the nuclearity of individual clusters.[17−20] Neumaier et al. have reported the kinetics of the reaction between the clusters $[Au_{25}(PET)_{18}]^-$ and $[Ag_{25}(DMBT)_{18}]^-$ in the solution.[21] This study has identified the formation of dimer species arising from cluster monomers in the course of the evolution of reactions and their existence points to important mechanistic details of the exchange processes.[21]

Supramolecular interactions between metal clusters have been utilized for the bottom-up fabrication of nanomaterials.[22−28] Directed self-assembly of clusters results in the formation of polymers of atomically precise clusters.[29−36] However, controlled self-assembly of clusters has been challenging, and Yuan et al. introduced a solvent-mediated approach for precisely synthesizing polymers of clusters.[37] In this work, we show that clusters can also interact with each other in the solid state, resulting in the exchange of metal atoms, which was not studied previously. In the solid state, the concentration of clusters is higher, favoring the adhesion between the clusters and consequently the metal atom exchange interactions, which could result in the formation of polymers of alloy metal clusters.

Specifically, we studied the polymerization that occurred due to metal atom exchange between $[Au_{25}(PET)_{18}]^-$ and $[Ag_{25}(DMBT)_{18}]^-$. We performed an experiment in which the powders of these two clusters were mixed in the solid state at various concentrations and times. Mass spectrometric analysis revealed the existence of species up to hexamers, which existed in the beginning. However, while performing mass spectrometry, the dilution in solution breaks the polymer, and eventually monomers exist in the solution. Time-dependent mass spectral analysis inferred that the kinetics of polymerization are faster in the solid state than in solution. The reaction studied using different ratios of the two clusters concluded that higher ratios of $[Au_{25}(PET)_{18}]^-$ enhanced metal exchange and favored polymerization. Insights from this

Received: May 9, 2024
Revised: June 19, 2024
Accepted: June 20, 2024

Downloaded via INDIAN INST OF TECH MADRAS on June 27, 2024 at 16:10:02 (UTC).
See https://pubs.acs.org/sharingguidelines for options on how to legitimately share published articles.

© XXXX American Chemical Society

work proposed a new pathway for developing self-assembled polymers of atomically precise alloy metal clusters by utilizing intercluster reactions in the solid state.

EXPERIMENTAL SECTION

Materials. All the materials were commercially available. Silver nitrate ($AgNO_3$), 2-phenylethanethiol (PET), 2,4-dimethylbenzenethiol (DMBT), tetraoctylammonium bromide (TOABr), tetraphenylphosphonium bromide (PPh_4Br), and sodium borohydride ($NaBH_4$) were purchased from Sigma-Aldrich. All the solvents, methanol, ethanol, acetone, chloroform, tetrahydrofuran, and dichloromethane, were purchased from Rankem. All solvents and chemicals were used as such without further purification.

Synthesis of $[Au_{25}(PET)_{18}]^-$. The $[Au_{25}(PET)_{18}]^-$ cluster was synthesized using the procedure reported previously.[16,38] The starting material, $HAuCl_4.3H_2O$, was synthesized in the lab by following the method presented in the Supporting Information. A quantity of 40 mg of $HAuCl_4.3H_2O$ (0.1 mmol) was taken in 7.5 mL of tetrahydrofuran. Then, 66.5 mg (0.116 mmol) of TOABr was added with continuous stirring. The solution changed from yellow to orange due to complexation. After 15 min of stirring, 68 μL of PET (C_8H_9SH) (0.53 mmol) was added. Gradually, the solution turned colorless. After 2 h of vigorous stirring, 40 mg of $NaBH_4$ (1 mmol) dissolved in 2 mL of ice-cold water was added rapidly. The stirring was continued for 8 h, and a reddish-brown solution was obtained as a crude product. After that, the reaction mixture was dried, and the black particles were collected. They were suspended in methanol, and the mixture was centrifuged at 5000 rpm for 3 min to collect all of the black precipitate completely. This was also done to remove any insoluble byproducts. The precipitate was washed 5 times with methanol to remove excess thiol. Then, the cluster was dissolved in 8 mL of dichloromethane and centrifuged at 10000 rpm for 5 min. The supernatant was collected and dried, and again, it was dissolved in acetone and centrifuged at 10000 rpm for 5 min. The acetone soluble fraction was collected, which is the required $[Au_{25}(PET)_{18}]^-$.

Synthesis of $[Ag_{25}(DMBT)_{18}]^-$. The $[Ag_{25}(DMBT)_{18}]^-$ cluster was synthesized by modifying the reported procedure.[39] Exactly 38 mg of $AgNO_3$ (0.22 mmol) was dissolved in a mixture of 2 mL of methanol and 17 mL of dichloromethane. Into this solution, 90 μL of DMBT (C_8H_9SH) (0.66 mmol) was added, which formed a yellow-colored suspension, and it was kept for stirring at 0 °C. After 20 min, a freshly prepared PPh_4Br (~6 mg, 0.014 mmol) solution in methanol (0.5 mL) was added with continued stirring. After 5 min, $NaBH_4$ (~15 mg, ~0.4 mmol) in 0.5 mL of ice-cold water was added. The color of the reaction mixture changed gradually from light yellow to dark brown. The solution was allowed to stir for 10 h and aged for 24 h in a freezer. The reaction mixture was centrifuged for purification of the cluster, and the supernatant was collected and concentrated to 5 mL. Excess methanol was added to the concentrated solution to precipitate the products. The obtained precipitate was washed multiple times (~5) with methanol. The precipitate was then dissolved in dichloromethane and centrifuged, and the supernatant was collected. The supernatant was dried, and the pure cluster was obtained in powder form.

Mixing of Clusters in the Solid State. The powders of both clusters $[Au_{25}(PET)_{18}]^-$ and $[Ag_{25}(DMBT)_{18}]^-$ were measured according to their molar ratio. Then, these clusters were mixed and ground using a mortar and pestle, in the laboratory environment. The clusters were mixed and ground for different time intervals (30 s, 1, 3, and 5 min), and the spectra were collected in each case. The ground mixture was dissolved in cold acetonitrile and held at −10 °C to minimize the solution phase contribution to the reaction. The sample was injected into the mass spectrometer within 30 s (retention time in solution), and the mass spectrum was acquired immediately. The entire mass spectral measurement, from sample preparation to data acquisition, was completed in 2 min. The same mixture was also analyzed using solid-state optical absorption measurements. In the further text, the reaction time corresponds to the grinding time of the two clusters.

RESULTS AND DISCUSSION

The clusters $[Au_{25}(PET)_{18}]^-$ and $[Ag_{25}(DMBT)_{18}]^-$ were chosen selectively based on their previous solution phase studies. Both clusters were synthesized as discussed in the Experimental Section. In the following text, the clusters $[Au_{25}(PET)_{18}]^-$ and $[Ag_{25}(DMBT)_{18}]^-$ will be represented as $Au_{25}(SR)_{18}$ and $Ag_{25}(SR)_{18}$, respectively. The protecting ligands of $Au_{25}(SR)_{18}$ and $Ag_{25}(SR)_{18}$ are 2-phenylethanethiol (PET) and 2,4-dimethylbenzenethiol (DMBT), respectively. These ligands were chosen due to their same molar masses (138 Da), which avoid complications due to ligand exchange between clusters in the course of metal exchange. Both clusters were synthesized and were further characterized by UV−vis absorption spectroscopy and electrospray ionization mass spectrometry (ESI-MS). The optical absorption spectra of both clusters exhibited their characteristic peaks, confirming their identity (Figure S1). The characteristic features of $Au_{25}(SR)_{18}$ were observed at 450 and 690 nm, whereas the characteristic peaks of $Ag_{25}(SR)_{18}$ were at 465, 495, 530, and 650 nm.[40] The ESI-MS of both clusters showed their characteristic peaks, with isotopic distribution matching the theoretical pattern (Figure S2). The peak of $Au_{25}(SR)_{18}$ was at m/z 7393 with a charge of 1-, whereas the peak of $Ag_{25}(SR)_{18}$ was at m/z 5167 with a charge of 1-. The clusters were mixed for different time intervals in powder form using a mortar and pestle, followed by ESI-MS measurements (Figure S4). The experiments were performed with different molar ratios of the $Au_{25}(SR)_{18}$ and $Ag_{25}(SR)_{18}$ clusters. The sample injection into the mass spectrometer was done quickly, within 1 min, to reduce the effect of solvent, and the data were collected within 2 min.

The mass spectrum obtained from the 1:1 molar ratio of $Ag_{25}(SR)_{18}$: $Au_{25}(SR)_{18}$, after mixing them for different time intervals, is presented in Figure 1a. In the mass spectrum, which was collected after 1 min of solid-state mixing, the characteristic features of $Au_{25}(SR)_{18}$ and $Ag_{25}(SR)_{18}$ were not observed. A new set of peaks was observed between m/z 5400 to 6000, and the zoomed-in spectra of this region are shown in Figure 1b. Each of the peaks in the isotopic distribution is separated by a m/z of less than 1, showing that these are highly charged species. The peaks observed in Figure 1b have monomer, dimer, and tetramer species, with 1-, 2-, and 4- charges, respectively. The mass separation between these peaks indicates a Au−Ag exchange between the two clusters. More detailed isotopically resolved spectra are not presented to confirm the exchange, although these have been presented in earlier reports.[21] Exchange between the ligands is not evident from the mass spectrum since the molecular masses of PET and DMBT ligands are the same. The monomeric metal-exchanged species were assigned as $Ag_{22}Au_3(SR)_{18}$ (m/z 5434), $Ag_{21}Au_4(SR)_{18}$ (m/z 5523), $Ag_{20}Au_5(SR)_{18}$ (m/z 5612), $Ag_{19}Au_6(SRS)_{18}$ (m/z 5701), $Ag_{18}Au_7(SR)_{18}$ (m/z 5790), $Ag_{17}Au_8(SR)_{18}$ (m/z 5879), $Ag_{16}Au_9(SR)_{18}$ (m/z 5968), and $Ag_{15}Au_{10}(SR)_{18}$ (m/z 6058) (nuclearity is always 25). Furthermore, the dimer species were identified as $Ag_{43}Au_7(SR)_{36}$ (m/z 5479), $Ag_{41}Au_9(SR)_{36}$ (m/z 5568), $Ag_{39}Au_{11}(SR)_{36}$ (m/z 5657), $Ag_{37}Au_{13}(SR)_{36}$ (m/z 5746), $Ag_{35}Au_{15}(SR)_{36}$ (m/z 5835), and $Ag_{33}Au_{17}(SR)_{36}$ (m/z 5925) (nuclearity is always 50). All of the dimer species observed were formed between metal-exchanged species. Notably, we have not observed the dimer formed between the pure parent clusters, $Ag_{25}(SR)_{18}$ and $Au_{25}(SR)_{18}$, which were present in the

https://doi.org/10.1021/acs.langmuir.4c01737
Langmuir XXXX, XXX, XXX−XXX

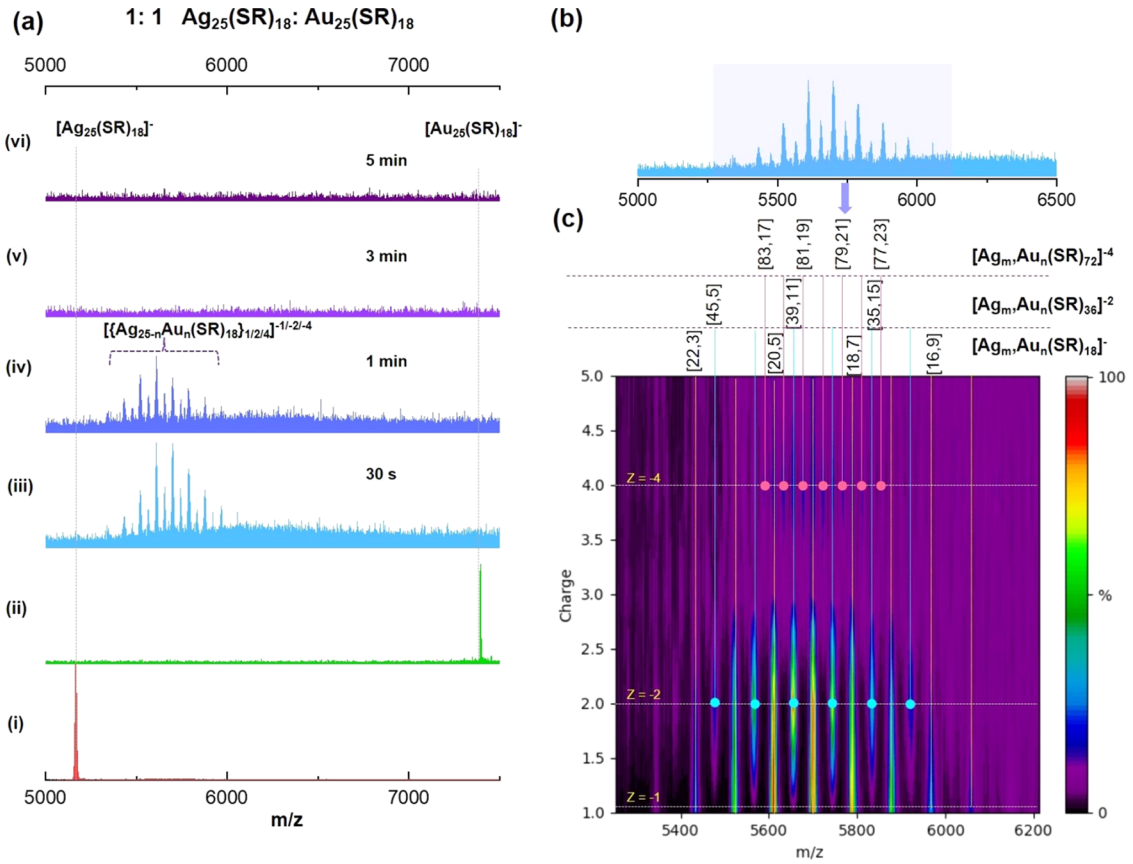

Figure 1. (a) ESI-MS of $Ag_{25}(SR)_{18}$, $Au_{25}(SR)_{18}$, and the time-dependent MS of the 1:1 mixture of $Ag_{25}(SR)_{18}$:$Au_{25}(SR)_{18}$ clusters measured after grinding the mixture. (b) Zoomed-in view of the mass spectrum collected after grinding the mixture for 1 min. (c) Heat map of the mass spectrum collected after grinding the mixture for 1 min (the compositions of various polymer species observed and their charge states marked).

previous report of solution phase intercluster reaction.[21] The tetramer peaks observed were due to $Ag_{83}Au_{17}(SR)_{72}$ (m/z 5545), $Ag_{81}Au_{19}(SR)_{72}$ (m/z 5590), $Ag_{79}Au_{21}(SR)_{72}$ (m/z 5634), and $Ag_{77}Au_{23}(SR)_{72}$ (m/z 5679) (nuclearity is always 100). The same peaks were observed in the mass spectrum collected after 3 min of solid-state grinding, but their intensities started to decrease with time. After 5 min of mixing, all of the peaks disappeared due to the degradation of clusters, presumably in the solution. The degraded products mostly consisted of metal thiolates and their exchanged species, which were assigned as $Ag_5(SR)_6$, $AuAg_4(SR)_6$, $Au_2Ag_3(SR)_6$, and $Au_3Ag_2(SR)_6$ (Figure S15).

We have performed the same experiment using different molar ratios, 1:1, 1:3, 3:1, 1:5, and 5:1 of $Ag_{25}(SR)_{18}$ and $Au_{25}(SR)_{18}$. The mass spectrum obtained for various molar ratios of the clusters after 1 min of solid-state mixing is presented in Figure 2a. As shown in Figure 1, the ratio 1:1 of $Ag_{25}(SR)_{18}$:$Au_{25}(SR)_{18}$ produced monomers, dimers, and tetramers of the exchanged species. In the mass spectra of 1:3 $Ag_{25}(SR)_{18}$:$Au_{25}(SR)_{18}$, the peaks for the parent clusters were observed. In the range of m/z 7250−7400, monomeric Ag exchanged peaks of $Au_{25}(SR)_{18}$ clusters were observed, while in the range of m/z 5200−5700, monomeric Au-exchanged peaks of $Ag_{25}(SR)_{18}$ were identified. The dimer peaks were also observed, but they were mainly concentrated in the range of m/z 7000, indicating that the contribution of Au atoms is more on the dimer, which accounts for the higher molar ratio of $Au_{25}(SR)_{18}$. The time-dependent mass spectra of 1:3 $Ag_{25}(SR)_{18}$:$Au_{25}(SR)_{18}$ show that metal exchange is happening within 30 s, and with an increase in time, the intensity of peaks decreases (Figure S3), indicating faster kinetics of the reaction. From the low-intensity peaks, we observed the presence of trimer species (3-), and their compositions were assigned as $Ag_6Au_{69}(SR)_{54}$ (m/z 7216), $Ag_3Au_{72}(SR)_{54}$ (m/z 7305), and $Au_{75}(SR)_{54}$ (m/z 7393). To further understand the low-intensity peaks, we made a heat map plot of the mass spectra (Figure S4), and surprisingly, we found the tetramers and pentamers of parent clusters $Ag_{25}(SR)_{18}$ and $Au_{25}(SR)_{18}$ (Figure S11). Similarly, in the mass spectra of the ratio 3:1 $Ag_{25}(SR)_{18}$:$Au_{25}(SR)_{18}$ also, the peaks for the parent clusters were observed. Time-dependent mass spectra (Figure S5) show that in the initial 1 min, only monomeric Au-exchanged peaks of $Ag_{25}(SR)_{18}$ clusters were formed in the range of m/z 5200−5500. However, with increase in time to 3 min, we observed excessive metal exchange between the clusters, and peaks were observed in the range of m/z 5800−6800 (Table S3). Furthermore, in the same range, we observed dimers, trimers, and tetramers of the metal-exchanged species (Figure S6 and Table S3). Besides that, at m/z 6324, a hexamer species $[Ag_{72}Au_{78}(SR)_{108}]^{6-}$ was found with the monomeric unit $[Ag_{12}Au_{13}(SR)_{18}]^{-}$, which was not previously reported (Figure S12). The mass spectral analysis showed that the kinetics of polymerization is slower in 3:1, compared to 1:3 $Ag_{25}(SR)_{18}$ and $Au_{25}(SR)_{18}$. Thus, we conclude that a higher ratio of $Au_{25}(SR)_{18}$ favors polymerization.

The time-dependent mass spectra of 1:5 $Ag_{25}(SR)_{18}$:$Au_{25}(SR)_{18}$ showed that the parent cluster peak

https://doi.org/10.1021/acs.langmuir.4c01737
Langmuir XXXX, XXX, XXX−XXX

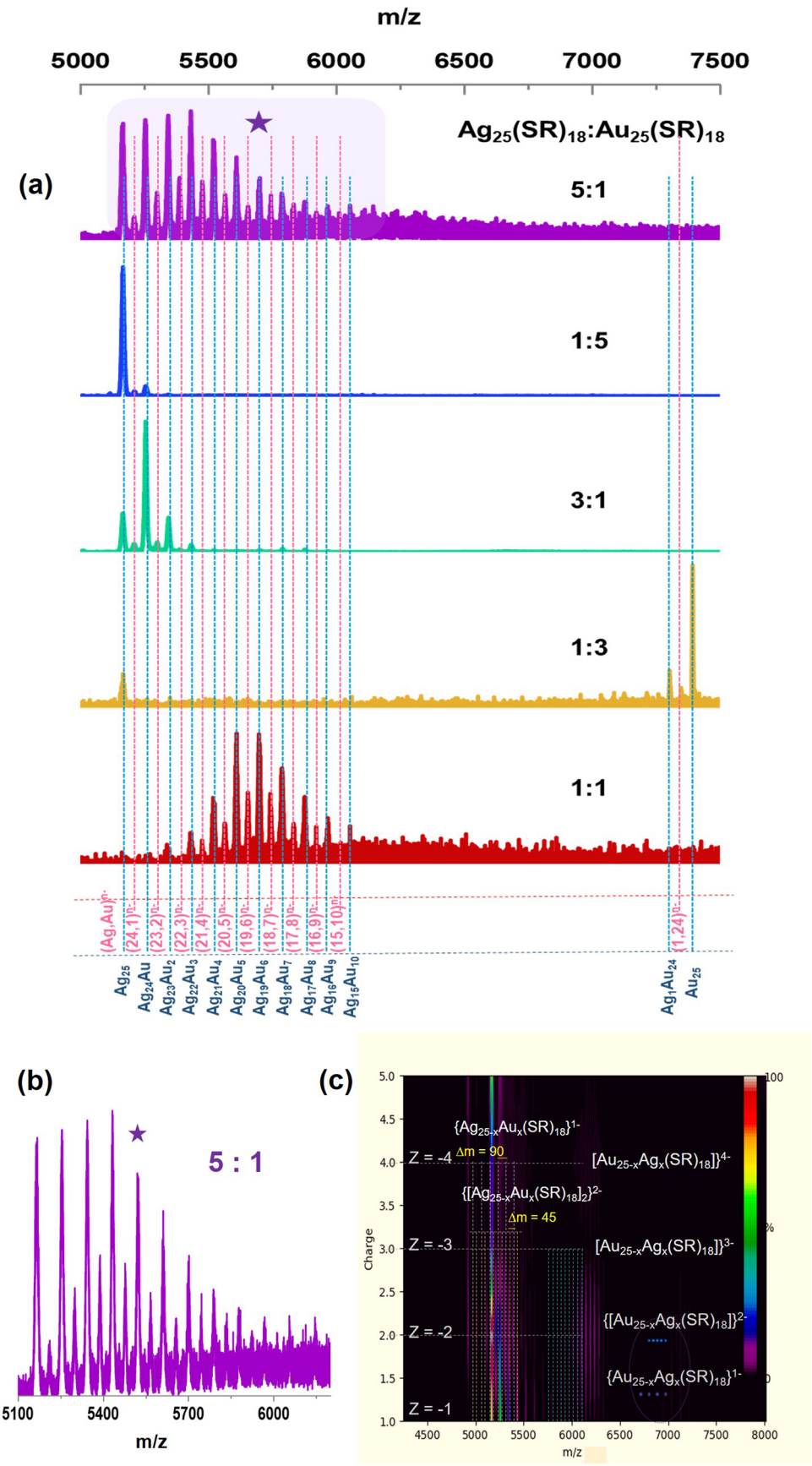

Figure 2. (a) ESI-MS, after 1 min of grinding, of a mixture of $Ag_{25}(SR)_{18}$ and $Au_{25}(SR)_{18}$ at various molar ratios. (b) Zoomed-in mass spectrum for the ratio 5:1 of $Ag_{25}(SR)_{18}$:$Au_{25}(SR)_{18}$. (c) Heat map plot for the ratio 5:1 of $Ag_{25}(SR)_{18}$:$Au_{25}(SR)_{18}$ (the compositions of various polymer species observed and their charge states are marked).

https://doi.org/10.1021/acs.langmuir.4c01737
Langmuir XXXX, XXX, XXX−XXX

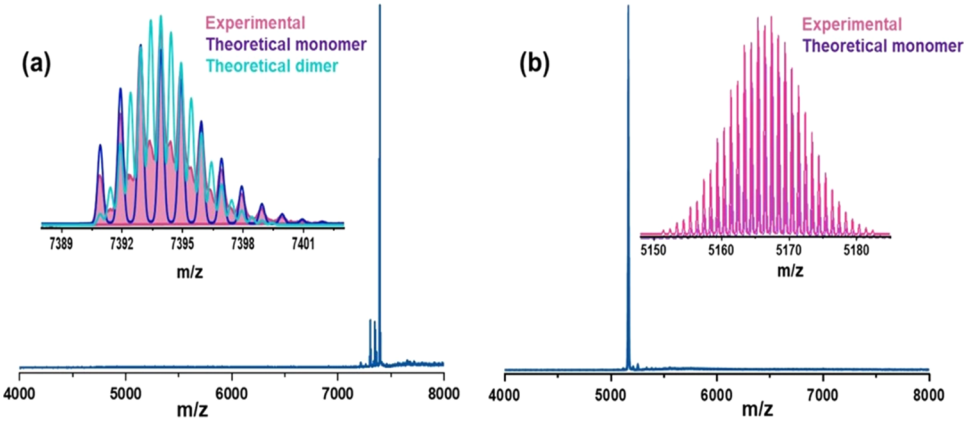

Figure 3. ESI-MS of (a) $Au_{25}(SR)_{18}$ and (b) $Ag_{25}(SR)_{18}$ measured after solid-state grinding. The inset shows the matching of the experimental and theoretical isotopic distributions. Dimers and trimers are marked in the inset of (a), and such species are not there in (b). Intensities of the theoretical monomer and dimer peaks were not matched with the experimental spectrum to make sure that the peaks were clearly visible.

of $Au_{25}(SR)_{18}$ was absent, even though the concentration was higher (Figure S7). Near m/z 5200, Au-exchanged peaks of $Ag_{25}(SR)_{18}$ were observed along with the less intense peaks around m/z 6000. The kinetics of the reaction were fast such that the peak intensity of the polymer species diminished rapidly. The heat map plot shows that low-intensity peaks around m/z 6000 consist of dimers, trimers, and tetramers (Figure S8), and their composition is presented in detail in Table S4. However, in the time-dependent mass spectra of 5:1 $Ag_{25}(SR)_{18}$:$Au_{25}(SR)_{18}$, the parent cluster peak of $Ag_{25}(SR)_{18}$ alone was present (Figure S9). Furthermore, the peaks of Au-exchanged species of $Ag_{25}(SR)_{18}$ were present, along with their dimer, trimer, and tetramer species (Figure S10). The polymer peaks were mainly concentrated near the range of m/z 5200−6000, attributed to the higher amount of $Ag_{25}(SR)_{18}$ present. The compositions of different polymer species formed are presented in Table S5. We observed from further analysis of the mass spectra that in the presence of higher amount of $Ag_{25}(SR)_{18}$, the polymers are concentrated toward lower m/z, whereas for higher amount of $Au_{25}(SR)_{18}$, they are found toward higher m/z values.

Metal atom exchange between the clusters is key for polymerization, which is evident from the mass spectrometry studies, and the polymeric species were formed by alloys. The analysis of mass spectra inferred that the presence of higher ratios of $Au_{25}(SR)_{18}$ favors the polymerization more compared to $Ag_{25}(SR)_{18}$, which is evident from the mass spectra of 1:1, 1:3, and 1:5 mixtures (Figure 2). To further explore this, we separately took both $Au_{25}(SR)_{18}$ and $Ag_{25}(SR)_{18}$ clusters in powder form, ground them separately using a mortar and pestle, and measured their mass spectra. This was done to understand the response of each cluster toward solid-state mixing. For $Au_{25}(SR)_{18}$, we observed dimers and trimers in the mass spectrum as seen before,[41] whereas for $Ag_{25}(SR)_{18}$, only monomers were present (Figure 3). This hinted at the tendency of $Au_{25}(SR)_{18}$ to form polymers, which corroborates our experimental results. The cluster $Ag_{25}(SR)_{18}$ alone could not form any polymer due to grinding, which further confirms that metal exchange between the two clusters is the driving force for polymerization.

We performed solid-state optical absorption measurements to confirm that interaction between clusters in the solid state is responsible for metal exchange and polymerization. We have taken equimolar amounts of clusters $Au_{25}(SR)_{18}$ and $Ag_{25}(SR)_{18}$ in the powder form, mixed them for different time intervals, and their corresponding absorption spectra were measured. The absorption spectra of individual clusters and the mixture at various time intervals are shown in Figure S13. The absorption spectra of parent clusters $Au_{25}(SR)_{18}$ and $Ag_{25}(SR)_{18}$ in the solid state measurements have shown some differences in the peaks compared to their solution phase data (Figure S1), which could be attributed to solvent effects. After mixing the clusters, the spectral features exhibited a notable shift in the peak positions compared to those of the parent clusters. However, the spectra collected at different time intervals of mixing did not show any prominent difference with respect to time. This suggests that the interaction between the clusters in the solid state is very fast and is completed within a few minutes, which matches well with the mass spectral analysis. The intensity of the absorption peaks also did not decrease even after 45 min of spectral measurement, indicating the stability of the cluster polymers in the solid state. We have also measured the time-dependent UV-vis absorption spectra of the ground mixture of clusters dissolved in cold acetonitrile at a time interval of 30 s and up to 2 min (Figure S14). These control experiments confirmed that the reaction is not very rapid upon dissolution in acetonitrile and that the effect of solvent was minimal on the mass spectral analysis.

The previous report on the solution phase reaction of $Au_{25}(SR)_{18}$ and $Ag_{25}(SR)_{18}$ showed that the dimer forms only after 3 min, and metal exchange happens later.[21] However, in the case of solid-state interaction, the reaction was more rapid than that in solution, and the whole reaction was completed within 5 min. In solution, the molecules will be far apart and have fewer chances of coming together, which is attributed to their slower kinetics. In solid-state mixing, the molecules are closer, which favors strong adhesion, and metal exchange happens between $Au_{25}(SR)_{18}$ and $Ag_{25}(SR)_{18}$ within the time scale of polymerization. The exchange efficiency of the two clusters $Ag_{25}(SR)_{18}$ and $Au_{25}(SR)_{18}$ in the solid state was nearly 100%. Time-dependent mass spectral analysis shows that initially, dimer species were forming, which further interacted with adjacent monomers or dimers to form oligomers. The polymeric species we have observed constitute both homopolymers and heteropolymers. Homopolymers have high-intensity peaks in the mass spectrum due to the overlap of the peaks of different species at the same m/z value. However, for heteropolymers, the peak intensities were found to be

https://doi.org/10.1021/acs.langmuir.4c01737
Langmuir XXXX, XXX, XXX−XXX

weaker. In the case of $Ag_{25}(SR)_{18}$:$Au_{25}(SR)_{18}$ ratio of 3:1, we observed an unprecedented hexamer species, and the theoretical agreement of the peak is shown in Figure S12.

The plausible mechanism for the polymerization of clusters can be (i) ligand−ligand interactions ($\pi\cdots\pi$, C−H$\cdots\pi$) and (ii) attractive van der Waals forces between the metal atoms and sulfur atoms in the staples of the interacting clusters. The aurophilic interactions[42] would also play a role, as is evident from the increased tendency of polymerization in the presence of more $Au_{25}(SR)_{18}$. A schematic representation of these interactions and the formation of polymers of metal clusters is shown in Figure 4. The negative charge on the cluster is

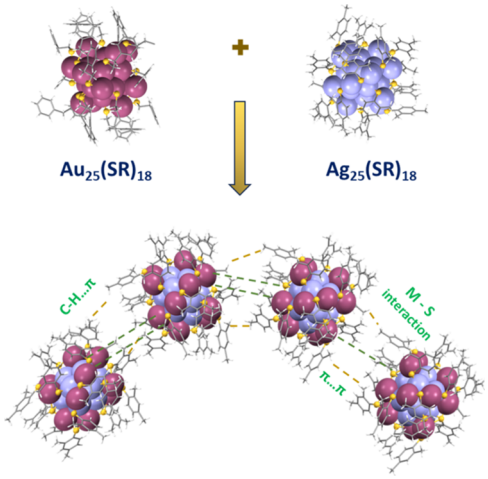

Figure 4. Schematic representation that demonstrates the formation of alloy cluster polymer from the parent clusters and interactions within the polymer.

delocalized throughout, electrostatic repulsion did not prevent intercluster interactions, as reported previously.[15] The counterions of $Au_{25}(SR)_{18}$ and $Ag_{25}(SR)_{18}$ are tetraoctylammonium (TOA^+) and tetraphenylphosphonium (Ph_4P^+), respectively, which are smaller compared to the size of metal clusters. Thus, the interference of counterions will be minimal during interaction between the clusters. The presence of $Au_{25}(SR)_{18}$ and its metal exchange with $Ag_{25}(SR)_{18}$ are crucial in the polymerization of clusters, which was evident from mass spectrometric observations. The grinding of the clusters also has a crucial role in the formation of alloy cluster polymers, since it promotes the interaction between clusters by providing energy. The mechanical energy from grinding provides the kinetic energy for the clusters to react with each other. As shown in Figure 3, the solid-state grinding of $Ag_{25}(SR)_{18}$ alone does not form polymers, implying that metal exchange between the clusters is the driving force for polymerization. Thus, intercluster reactions turn out to be a plausible strategy for synthesizing polymers of atomically precise alloy metal clusters.

CONCLUSIONS

In conclusion, we report the polymerization of atomically precise metal clusters due to metal exchange in the solid state. The interaction between electronically stable and geometrically robust metal clusters $[Au_{25}(PET)_{18}]^-$ and $[Ag_{25}(DMBT)_{18}]^-$ in the solid state produced dimers (2-), trimers (3-), tetramers (4-), pentamers (5-), and hexamers (6-), which were not reported earlier. This interaction can synthesize controlled polymers of bimetallic Ag−Au clusters with the desired number of monomeric units by optimizing the ratios of the reactant clusters. The kinetics of the reaction are faster compared to the already known solution phase studies, and the metal exchange between the clusters favors the polymerization. We observed that higher ratios of $Au_{25}(SR)_{18}$ have faster kinetics for polymerization than higher ratios of $Ag_{25}(SR)_{18}$. Mass spectrometry revealed the existence of polymers up to hexamers with a 6- charge, but other higher oligomers could also be present, which were not observed due to their weak intensities. Extension of this study using other metal clusters would provide more insights into the mechanism and help generalize this approach to synthesize polymers of atomically precise alloy metal clusters.

ASSOCIATED CONTENT

Supporting Information

The Supporting Information is available free of charge at https://pubs.acs.org/doi/10.1021/acs.langmuir.4c01737.

ESI mass spectra, UV−vis absorption spectra, and heat map plots (PDF)

AUTHOR INFORMATION

Corresponding Author

Thalappil Pradeep − *Department of Chemistry, DST Unit of Nanoscience (DST UNS) and Thematic Unit of Excellence (TUE), Indian Institute of Technology Madras, Chennai 600036, India; International Centre for Clean Water, Chennai 600113, India;* orcid.org/0000-0003-3174-534X; Email: pradeep@iitm.ac.in

Authors

B. S. Sooraj − *Department of Chemistry, DST Unit of Nanoscience (DST UNS) and Thematic Unit of Excellence (TUE), Indian Institute of Technology Madras, Chennai 600036, India;* orcid.org/0000-0002-6963-6491

Jayoti Roy − *Department of Chemistry, DST Unit of Nanoscience (DST UNS) and Thematic Unit of Excellence (TUE), Indian Institute of Technology Madras, Chennai 600036, India*

Manish Mukherjee − *Department of Chemistry, DST Unit of Nanoscience (DST UNS) and Thematic Unit of Excellence (TUE), Indian Institute of Technology Madras, Chennai 600036, India; Department of Chemistry, Indian Institute of Science Education and Research Kolkata, Kolkata 741246, India*

Anagha Jose − *Department of Chemistry, DST Unit of Nanoscience (DST UNS) and Thematic Unit of Excellence (TUE), Indian Institute of Technology Madras, Chennai 600036, India*

Complete contact information is available at: https://pubs.acs.org/10.1021/acs.langmuir.4c01737

Author Contributions

‖B.S.S. and J.R. contributed equally to this work. B.S.S. performed the synthesis, characterization, and other experimental studies. J.R. performed the mass spectrometry studies. M.M. and A.J. performed the synthesis and characterization of clusters. B.S.S. wrote the first draft with inputs from J.R. T.P. has conceptualized the work, directed the progress, and edited the final version of the manuscript. All authors have approved the final version of the manuscript.

https://doi.org/10.1021/acs.langmuir.4c01737
Langmuir XXXX, XXX, XXX−XXX

Notes

The authors declare no competing financial interest.

■ ACKNOWLEDGMENTS

B.S.S. thanks the Council of Scientific & Industrial Research (CSIR) for the SPM research fellowship. J.R. thanks IIT Madras for a research fellowship. M.M. thanks Kishore Vaigyanik Protsahan Yojana (KVPY) programme and IISER Kolkata for funding. A.J. thanks MHRD for the Prime Minister's Research Fellowship (PMRF). T.P. thanks the Science and Engineering Research Board (SERB), India, for funding through the research grant SPR/2021/000439 and through a JC Bose Fellowship. T.P. also acknowledges funding from the Centre of Excellence on Molecular Materials and Functions under the Institution of Eminence scheme of IIT Madras. We thank the Department of Science and Technology, Government of India, for continuous support of our research program.

■ DEDICATION

This article is dedicated to Prof. Santanu Bhattacharya on the occasion of his 65th birthday.

■ REFERENCES

(1) Jin, R.; Zeng, C.; Zhou, M.; Chen, Y. Atomically Precise Colloidal Metal Nanoclusters and Nanoparticles: Fundamentals and Opportunities. *Chem. Rev.* **2016**, *116* (18), 10346−10413.

(2) Lu, Y.; Chen, W. Sub-Nanometre Sized Metal Clusters: From Synthetic Challenges to the Unique Property Discoveries. *Chem. Soc. Rev.* **2012**, *41* (9), 3594−3623.

(3) Jin, R. Quantum Sized, Thiolate-Protected Gold Nanoclusters. *Nanoscale* **2010**, *2* (3), 343−362.

(4) Templeton, A. C.; Wuelfing, W. P.; Murray, R. W. Monolayer-Protected Cluster Molecules. *Acc. Chem. Res.* **2000**, *33* (1), 27−36.

(5) Ferrando, R.; Jellinek, J.; Johnston, R. L. Nanoalloys: From Theory to Applications of Alloy Clusters and Nanoparticles. *Chem. Rev.* **2008**, *108*, 845−910.

(6) Chakraborty, I.; Pradeep, T. Atomically Precise Clusters of Noble Metals: Emerging Link between Atoms and Nanoparticles. *Chem. Rev.* **2017**, *117* (12), 8208−8271.

(7) Li, S.; Li, N. N.; Dong, X. Y.; Zang, S. Q.; Mak, T. C. W. Chemical Flexibility of Atomically Precise Metal Clusters. *Chem. Rev.* **2024**, *124*, 7262.

(8) Zou, X.; Kang, X.; Zhu, M. Recent Developments in the Investigation of Driving Forces for Transforming Coinage Metal Nanoclusters. *Chem. Soc. Rev.* **2023**, *52* (17), 5892−5967.

(9) Zhu, M.; Aikens, C. M.; Hendrich, M. P.; Gupta, R.; Qian, H.; Schatz, G. C.; Jin, R. Reversible Switching of Magnetism in Thiolate-Protected Au_{25} Superatoms. *J. Am. Chem. Soc.* **2009**, *131* (7), 2490−2492.

(10) Wang, X.; Zhao, L.; Li, X.; Liu, Y.; Wang, Y.; Yao, Q.; Xie, J.; Xue, Q.; Yan, Z.; Yuan, X.; Xing, W. Atomic-Precision Pt_6 Nanoclusters for Enhanced Hydrogen Electro-Oxidation. *Nat. Commun.* **2022**, *13* (1), No. 1596.

(11) Jin, R. Atomically Precise Metal Nanoclusters: Stable Sizes and Optical Properties. *Nanoscale* **2015**, *7* (5), 1549−1565.

(12) Jose, A.; Jana, A.; Gupte, T.; Nair, A. S.; Unni, K.; Nagar, A.; Kini, A. R.; Spoorthi, B. K.; Jana, S. K.; Pathak, B.; Pradeep, T. Vertically Aligned Nanoplates of Atomically Precise Co_6S_8 Cluster for Practical Arsenic Sensing. *ACS Mater. Lett.* **2023**, *5* (3), 893−899.

(13) Wang, S.; Song, Y.; Jin, S.; Liu, X.; Zhang, J.; Pei, Y.; Meng, X.; Chen, M.; Li, P.; Zhu, M. Metal Exchange Method Using Au_{25} Nanoclusters as Templates for Alloy Nanoclusters with Atomic Precision. *J. Am. Chem. Soc.* **2015**, *137* (12), 4018−4021.

(14) Baksi, A.; Schneider, E. K.; Weis, P.; Krishnadas, K. R.; Ghosh, D.; Hahn, H.; Pradeep, T.; Kappes, M. M. Nanogymnastics: Visualization of Intercluster Reactions by High-Resolution Trapped Ion Mobility Mass Spectrometry. *J. Phys. Chem. C* **2019**, *123* (46), 28477−28485.

(15) Krishnadas, K. R.; Ghosh, A.; Baksi, A.; Chakraborty, I.; Natarajan, G.; Pradeep, T. Intercluster Reactions between $Au_{25}(SR)_{18}$ and $Ag_{44}(SR)_{30}$. *J. Am. Chem. Soc.* **2016**, *138* (1), 140−148.

(16) Krishnadas, K. R.; Baksi, A.; Ghosh, A.; Natarajan, G.; Pradeep, T. Manifestation of Geometric and Electronic Shell Structures of Metal Clusters in Intercluster Reactions. *ACS Nano* **2017**, *11* (6), 6015−6023.

(17) Huang, B.; Pei, Y. On the Mechanism of Inter-Cluster Alloying Reactions: Two-Stage Metal Exchange of $[Au_{25}(PET)_{18}]^-$ and $[Ag_{25}(DMBT)_{18}]^-$ Clusters. *J. Mater. Chem. A* **2020**, *8* (20), 10242−10251.

(18) Zhang, B.; Salassa, G.; Bürgi, T. Silver Migration between $Au_{38}(SC_2H_4Ph)_{24}$ and Doped $Ag_XAu_{38-x}(SC_2H_4Ph)_{24}$ Nanoclusters. *Chem. Commun.* **2016**, *52* (59), 9205−9207.

(19) Krishnadas, K. R.; Baksi, A.; Ghosh, A.; Natarajan, G.; Pradeep, T. Structure-Conserving Spontaneous Transformations between Nanoparticles. *Nat. Commun.* **2016**, *7*, No. 13447.

(20) Krishnadas, K. R.; Baksi, A.; Ghosh, A.; Natarajan, G.; Som, A.; Pradeep, T. Interparticle Reactions: An Emerging Direction in Nanomaterials Chemistry. *Acc. Chem. Res.* **2017**, *50* (8), 1988−1996.

(21) Neumaier, M.; Baksi, A.; Weis, P.; Schneider, E. K.; Chakraborty, P.; Hahn, H.; Pradeep, T.; Kappes, M. M. Kinetics of Intercluster Reactions between Atomically Precise Noble Metal Clusters $[Ag_{25}(DMBT)_{18}]^-$ and $[Au_{25}(PET)_{18}]^-$ in Room Temperature Solutions. *J. Am. Chem. Soc.* **2021**, *143* (18), 6969−6980.

(22) De Nardi, M.; Antonello, S.; Jiang, D. E.; Pan, F.; Rissanen, K.; Ruzzi, M.; Venzo, A.; Zoleo, A.; Maran, F. Gold Nanowired: A Linear $(Au_{25})_n$ Polymer from Au_{25} Molecular Clusters. *ACS Nano* **2014**, *8* (8), 8505−8512.

(23) Qiao, Y.; Zou, J.; Fei, W.; Fan, W.; You, Q.; Zhao, Y.; Li, M. B.; Wu, Z. Building Block Metal Nanocluster-Based Growth in 1D Direction. *Small* **2023**, *20* (9), No. 2305556.

(24) Lahtinen, T.; Hulkko, E.; Sokołowska, K.; Tero, T. R.; Saarnio, V.; Lindgren, J.; Pettersson, M.; Häkkinen, H.; Lehtovaara, L. Covalently Linked Multimers of Gold Nanoclusters $Au_{102}(pMBA)_{44}$ and $Au_{\sim 250}(pMBA)_n$. *Nanoscale* **2016**, *8* (44), 18665−18674.

(25) Lei, Z.; Li, J. J.; Nan, Z. A.; Jiang, Z. G.; Wang, Q. M. Cluster From Cluster: A Quantitative Approach to Magic Gold Nanoclusters $[Au_{25}(SR)_{18}]^-$. *Angew. Chem., Int. Ed.* **2021**, *60* (26), 14415−14419.

(26) Ito, E.; Takano, S.; Nakamura, T.; Tsukuda, T. Controlled Dimerization and Bonding Scheme of Icosahedral $M@Au_{12}$ (M = Pd, Pt) Superatoms. *Angew. Chem., Int. Ed.* **2021**, *60* (2), 645−649.

(27) Dainese, T.; Antonello, S.; Bogialli, S.; Fei, W.; Venzo, A.; Maran, F. Gold Fusion: From $Au_{25}(SR)_{18}$ to $Au_{38}(SR)_{24}$, the Most Unexpected Transformation of a Very Stable Nanocluster. *ACS Nano* **2018**, *12* (7), 7057−7066.

(28) Tang, L.; Kang, X.; Wang, S.; Zhu, M. Light-Induced Size-Growth of Atomically Precise Nanoclusters. *Langmuir* **2019**, *35* (38), 12350−12355.

(29) Liu, X.; Saranya, G.; Huang, X.; Cheng, X.; Wang, R.; Chen, M.; Zhang, C.; Li, T.; Zhu, Y. $Ag_2Au_{50}(PET)_{36}$ Nanocluster: Dimeric Assembly of $Au_{25}(PET)_{18}$ Enabled by Silver Atoms. *Angew. Chem., Int. Ed.* **2020**, *59* (33), 13941−13946.

(30) Alhilaly, M. J.; Huang, R. W.; Naphade, R.; Alamer, B.; Hedhili, M. N.; Emwas, A. H.; Maity, P.; Yin, J.; Shkurenko, A.; Mohammed, O. F.; Eddaoudi, M.; Bakr, O. M. Assembly of Atomically Precise Silver Nanoclusters into Nanocluster-Based Frameworks. *J. Am. Chem. Soc.* **2019**, *141* (24), 9585−9592.

(31) Wang, Z. Y.; Wang, M. Q.; Li, Y. L.; Luo, P.; Jia, T. T.; Huang, R. W.; Zang, S. Q.; Mak, T. C. W. Atomically Precise Site-Specific Tailoring and Directional Assembly of Superatomic Silver Nanoclusters. *J. Am. Chem. Soc.* **2018**, *140* (3), 1069−1076.

(32) Liu, Y.; Yao, D.; Zhang, H. Self-Assembly Driven Aggregation-Induced Emission of Copper Nanoclusters: A Novel Technology for Lighting. *ACS Appl. Mater. Interfaces* **2018**, *10* (15), 12071−12080.

https://doi.org/10.1021/acs.langmuir.4c01737
Langmuir XXXX, XXX, XXX−XXX

(33) Liu, J.; Tian, Y.; Ai, L.; Wu, Z.; Yao, D.; Liu, Y.; Yang, B.; Zhang, H. Self-Assembly of Au Nanoclusters into Helical Ribbons by Manipulating the Flexibility of Capping Ligands. *Langmuir* **2020**, *36* (48), 14614−14622.
(34) Fu, J.; Miao, Y.; Zhang, D.; Zhang, Y.; Meng, L.; Ni, X.; Shen, J.; Qi, W. Polymer-Enabled Assembly of Au Nanoclusters with Luminescence Enhancement and Macroscopic Chirality. *Langmuir* **2023**, *39* (37), 13316−13324.
(35) Wang, Y. X.; Li, A. J.; Wang, H. L.; Liu, W.; Kang, J.; Lu, J.; Lu, S. Y.; Yang, Y.; Liu, K.; Yang, B. In Situ Seed-Mediated Growth of Polymer-Grafted Gold Nanoparticles. *Langmuir* **2020**, *36* (3), 789−795.
(36) Kauscher, U.; Penders, J.; Nagelkerke, A.; Holme, M. N.; Nele, V.; Massi, L.; Gopal, S.; Whittaker, T. E.; Stevens, M. M. Gold Nanocluster Extracellular Vesicle Supraparticles: Self-Assembled Nanostructures for Three-Dimensional Uptake Visualization. *Langmuir* **2020**, *36* (14), 3912−3923.
(37) Yuan, P.; Zhang, R.; Selenius, E.; Ruan, P.; Yao, Y.; Zhou, Y.; Malola, S.; Häkkinen, H.; Teo, B. K.; Cao, Y.; Zheng, N. Solvent-Mediated Assembly of Atom-Precise Gold−Silver Nanoclusters to Semiconducting One-Dimensional Materials. *Nat. Commun.* **2020**, *11* (1), No. 2229.
(38) Heaven, M. W.; Dass, A.; White, P. S.; Holt, K. M.; Murray, R. W. Crystal Structure of the Gold Nanoparticle $[N(C_8H_{17})_4][Au_{25}(SCH_2CH_2Ph)_{18}]$. *J. Am. Chem. Soc.* **2008**, *130* (12), 3754−3755.
(39) Joshi, C. P.; Bootharaju, M. S.; Alhilaly, M. J.; Bakr, O. M. $[Ag_{25}(SR)_{18}]^-$: The "Golden" Silver Nanoparticle Silver Nanoparticle. *J. Am. Chem. Soc.* **2015**, *137* (36), 11578−11581.
(40) Sooraj, B. N. S.; Pradeep, T. Optical Properties of Metal Clusters. In *Atomically Precise Metal Nanoclusters*; Elsevier, 2023; pp 83−101.
(41) Baksi, A.; Chakraborty, P.; Bhat, S.; Natarajan, G.; Pradeep, T. $[Au_{25}(SR)_{18}]_2^{2-}$: A Noble Metal Cluster Dimer in the Gas Phase. *Chem. Commun.* **2016**, *52* (54), 8397−8400.
(42) Schmidbaur, H.; Schier, A. Aurophilic Interactions as a Subject of Current Research: An up-Date. *Chem. Soc. Rev.* **2012**, *41* (1), 370−412.

https://doi.org/10.1021/acs.langmuir.4c01737
Langmuir XXXX, XXX, XXX−XXX